Wire Bond Temperature Sensor

Shivesh Suman, Michael Gaitan*, Yogendra Joshi, George Harman*
University of Maryland, College Park, MD 20742
*National Institute of Standards and Technology
Semiconductor Electronics Division, Gaithersburg, MD 2089
Fax 301-948-4081 Tel. 301-484-0724, e-mail: shivesh@glue.umd.edu

Abstract

This work reports the first demonstration of a bond pad test structure with embedded thermopile sensors for the measurement of the transient temperature response during the wire bonding operation. This paper will present the design and operation of the bond pad test structure and show and discuss temperature measurements during the wire bonding operation. The test structure can be used directly on the bond pads without any modification to the bonding machine or imposition of constraints on the wire material. The thermocouple junctions are created by the aluminum-polysilicon contacts that are available in the standard CMOS process. This configuration does not require an external bias for the detector, as has been utilized in other studies. The test structure can be used in industrial applications for testing and calibrating wire bonding tools. Researchers can also use it as a probe for validating physics-based models of the wire bonding process. The device has been used for measuring the temperature response during ball bonding using 25 μm diameter gold wire. Measurements are reported for selected force and ultrasonic power settings and show generally expected trends. The sensor captures the cooling of the bond-pad by the gold ball and the heating due to the ultrasonic energy application. The results of this study are in qualitative agreement with a previous study using resistive temperature sensors.

Keywords: Gold ball bonding, CMOS compatible MEMS, thermocouple temperature sensor, Seebeck effect.

Introduction

Ball bonding remains the most commonly used interconnection technology. Extensive research on the mechanism of bond formation has not resulted in a comprehensive physics-based model of the physical process. The large number of parameters involved in the bonding process and a lack of the quantitative understanding of the ultrasonic softening [1] makes the optimization of the wire bonding operation difficult. The amount of heating that occurs during the wire bonding process and whether the heat generated during the process affects the quality of the bond are sources of argument. Recently several researchers have reported the transient temperature variation during the wire bonding process at a distance of a few micrometers away from the bonding interface [2,3,4].

Characterization of the bond interface reveals that the bonding is caused by the growth of inter-metallic compounds at discrete locations rather than throughout the interface [1]. This paper presents the development of a novel thermopile device located under the pad, which allows the measurement of temperature at certain points under the bond pad. This can be indirectly used for optimization of the bonding process, as suggested by other researchers [2].

Temperature Sensor

Figure 1 shows the schematic of the test structure. It consists of a thermopile with twenty-four aluminum-polysilicon thermocouples connected in series. The polysilicon is heavily doped n-type. All the cold junctions are located under the pad and the hot junctions are away from the pad. The junctions under the bond pad undergo a change in temperature during the bonding process, compared to the junctions further away. The difference in temperature between the junctions under the pad and the junctions further away is measured by the voltage across the series of thermocouples constituting the thermopile. The device is made in a standard CMOS process. The Seebeck coefficient of the aluminum-polysilicon thermoelectric junction is measured using another device located on the same chip as the thermopile structures. This device and the measurement technique for the Seebeck coefficient are based on the principle reported in [7]. The Seebeck coefficient of one thermocouple was measured to be 50 μV/°C.

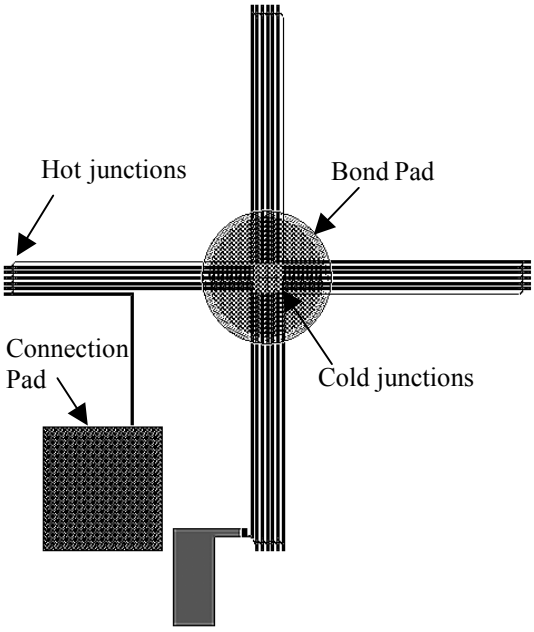

Fig. 1 Layout of the temperature sensor. Each arm consists of six thermocouple pairs connected in series and the four arms are connected in series to form the thermopile.

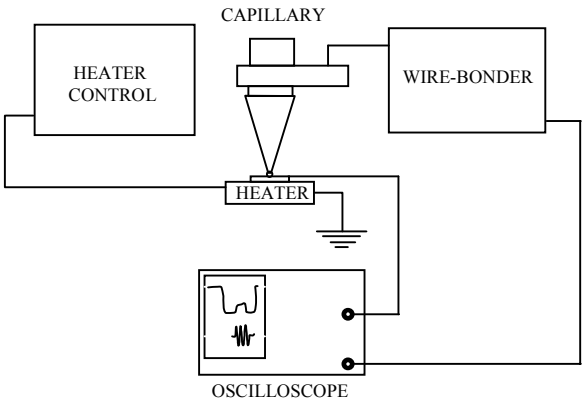

Fig. 2 Schematic of the experimental setup. The chip is kept at 150 °C by the heater control. The oscilloscope captures the transient Seebeck voltage on application of ultrasonic. The heater stage is grounded to reduce the noise in signal.

Experimental Setup

Figure 2 shows the schematic layout of the experimental setup. A Kulicke & Soffa 4124 NEFO, manual bonder with a 25 µm gold wire, is used for making the bond. The measurements are made while actually making a bond on the bond pad. The output from the thermopile is read using a digital oscilloscope. The application of ultrasonic energy is used as the trigger for the oscilloscope. Thus, a transient temperature profile during the wire bonding process is obtained. The measured voltage is converted into the equivalent temperature difference by multiplying it with the measured value of the Seebeck coefficient.

The thermocouple junctions are located directly below the bond pad. A 0.5 µm thick layer of passivation insulates the bond pad and the thermopile junctions. The measured temperature is expected to be close to the interface temperature. The resistance of each device was measured before and after making the bond to confirm that the junctions below the pad were not damaged during bonding.

Figure 3 shows a sample output of the thermocouple. Formation of the ball bond is represented in three stages. In stage (a), the capillary comes down and touches the bond pad and there is a steep drop in the temperature of the bond-pad due to local cooling by the ball and the capillary. The thermopile captures the instantaneous cooling of pad. This indicates that the time constant of the device is adequate for the purpose of the present measurements. After the initial cooling, the temperature of the bond pad recovers partially due to the flow of heat from the heated chip to the capillary. Stage (b) represents the application of ultrasonic energy and is accompanied by an initial rise in temperature, followed by a peak in temperature while the ultrasonic excitation is on, and a steep drop in temperature as soon as the ultrasonic excitation stops. Stage (b) is of particular interest since the bond formation takes place during this period. Stage (c) occurs after the bond has already formed and the capillary is still touching the bond pad without an ultrasonic excitation. During this stage, the temperature remains constant and returns to its initial level after the tool lifts off. Similar temperature variations have been reported earlier [2]. In order to make sure that the measurements are not affected by the parasitic piezoelectric output of the thermopile, bonds were made without heating the chip, and no response was obtained when the ball came in contact with the pad. Therefore, we assume that the output of the device is only due to the Seebeck effect and is proportional to the difference in the temperature of the hot and cold junctions of the thermopile.

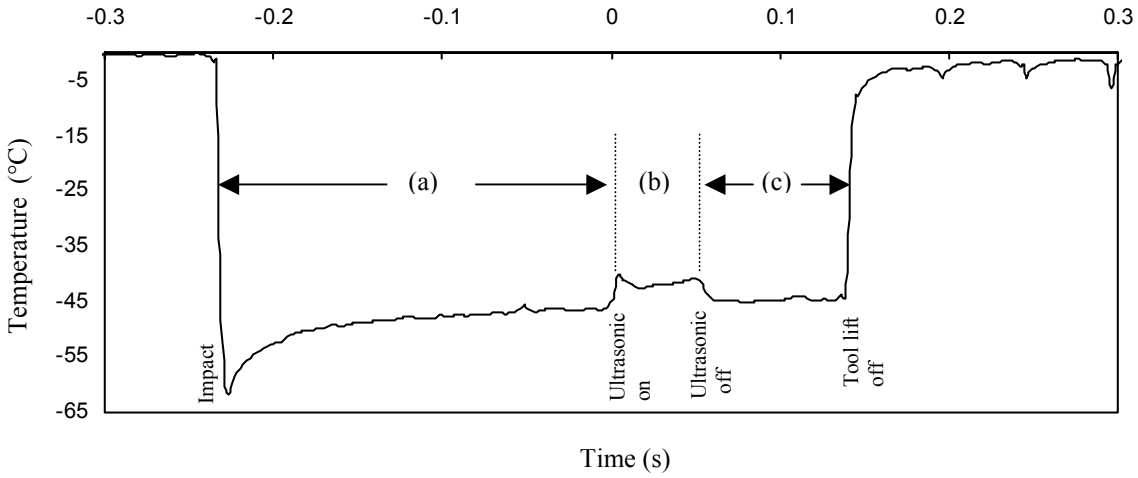

Fig. 3 A sample thermal response of the thermocouple during the ball bonding operation. (a) Cooling due to touchdown of the capillary and temperature recovery. (b) Heating due to the ultrasonic excitation. (c) Cooling after the ultrasonic energy is switched off followed by the tool lift off.

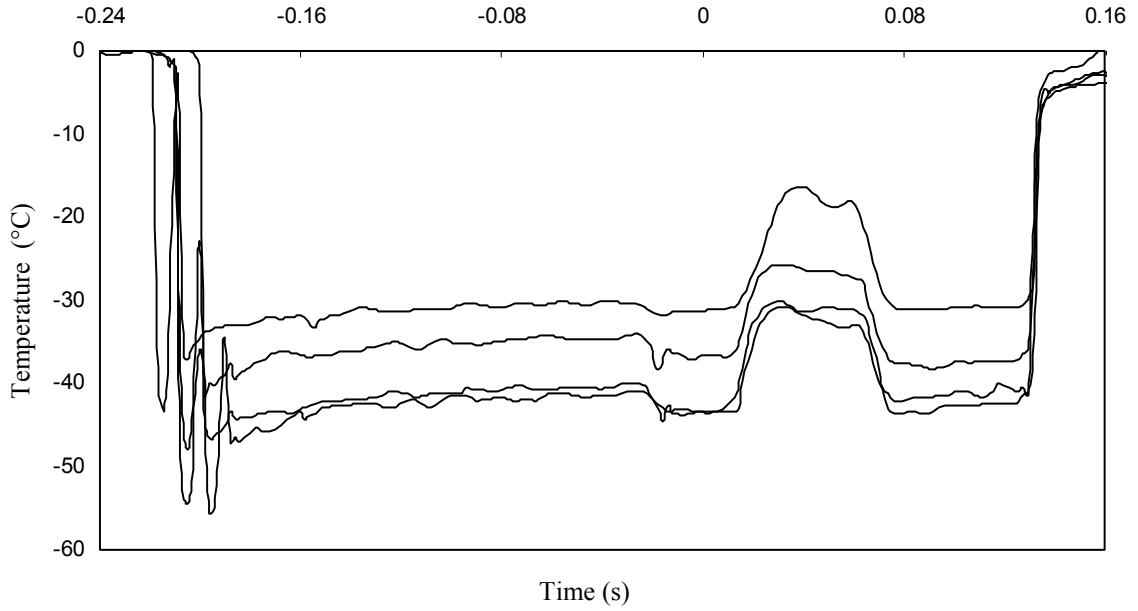

Fig. 4 A set of data for the wire thermal response of the thermocouple during bonding for a bonding force of 0.78 N and an input power of 0.37 W.

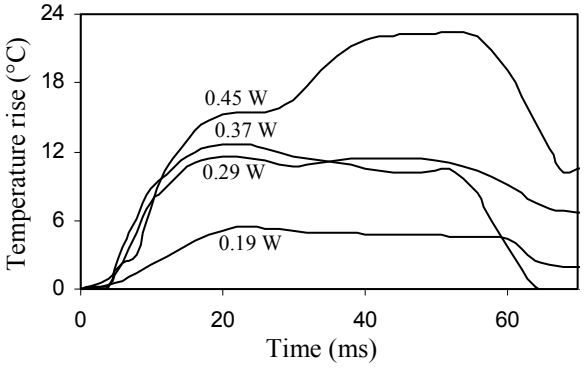

Fig. 5 Temperature rise due to application of ultrasonic energy for four different input powers at a bonding force of 0.78 N.

Experimental Results

Measurements were taken at different power settings at two values of bonding forces. Figure 4 shows a data set for a bonder force setting of 0.78 N and an input ultrasonic power of 0.37 W. The initial cooling of the bond pad is equivalent to two semi-infinite bodies at different temperatures coming in contact. The noise at the touchdown could be due to rebound of the capillary on the bond pad. The variability in the readings is attributed to the non-planarity of the bond pad and manual bonding operation. A small misalignment results in a different contact area due to the non-planarity of the surface. This results in a different value of thermal contact resistance for every pad. Also, the temperature read by the device is sensitive to the placement of the bond on the pad. The heating of the bond interface is estimated by reading the increase in temperature after the ultrasonic excitation is applied.

Figure 5 shows the ultrasonic heating for different power levels at a bonder force setting of 0.78 N. During the first few milliseconds of the ultrasonic excitation, the ball scrubs on the pad. The increase in the temperature might be due to the energy generated due to friction at the ball and pad interface [4] . A decrease in temperature after about 20 ms apparently indicates pinning of the ball and growth of the micro-welds. The bond formation is accompanied with the deformation of the ball due to ultrasonic softening [1]. The deformation of the ball and the growth of micro-welds result in a greater area of contact, and this results in a decrease in interface temperature after the initial peak. The slope of the temperature profile during the first ten millisecond increases with an increase in ultrasonic power for a fixed bonding force. A similar trend was observed at a bonding force of 0.82 N.

Modeling

A two-dimensional finite element heat conduction model for the first two stages of the bonding process was developed using ANSYS. The main objective of the present modeling is to get a qualitative variation of temperature for the first two stages of the bonding. The extent of the domain was selected based on the one-dimensional thermal penetration depth for aluminum, silicon, and gold. The material properties used in the model are listed in Table 1. The one-dimensional thermal penetration depth is computed as twice the square root of the product of thermal diffusivity and time. The radius and height of the silicon block are taken as 2.5 mm, which is the penetration depth for silicon in one dimension. Penetration depth in the present case is expected to be much less due to the three dimensional spreading of heat. The capillary is modeled with its actual height of 10 mm. The sensor is lumped with silicon since the thermal diffusivity for aluminum and silicon are close, and the thickness of the sensor is small compared to the computational domain. The model does not include the transient deformation and change in the shape of the ball or the contact resistance between the ball and the bond pad. The ball is modeled as shown in figure 6. The diameter of ball footprint is taken as 75 μm. An air gap of 25 μm is taken between the wire and the capillary. Axi-symmetric, quadrilateral elements were used for discritizing the domain. Figure 7 shows the mesh near the ball and bond pad interface.

Table 1 Material properties used in the conduction model.

	Thermal Conductivity (W/m.K)	Heat Capacity (J/Kg.K)	Density (Kg/m^3)
Capillary (Alumina)	12	1109	4005
Chip (silicon)	157	702	2330
Air	0.027	1005	1.12
Gold	313	129	19302

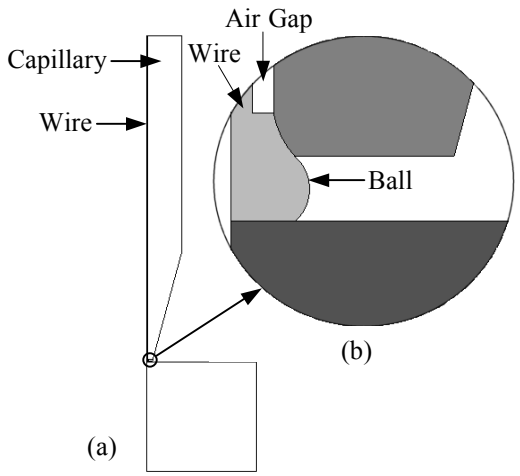

Fig. 6 (a) Geometry of the capillary, ball, wire, and air gap used in the model. (b) Geometry of the ball. Ball and capillary are taken at room temperature (22°C) and chip is taken at a uniform temperature of 150 °C at t=0. All boundaries are taken as insulated.

Heating due to the application of ultrasonic energy is modeled as a surface heat source at the interface between the ball and chip. The surface heat load is spread as a uniform heat input of 0.11 W over the area of contact between the ball and the bond pad. Figure 8 shows the variation in temperature as a function of time at (a) the center of the bond pad and (b) a radial distance of 250 μm (far end of the thermocouple), for a touchdown period of 240 ms, followed by a surface heating for 65 ms. The surface heat source is set to zero at t=305 ms. The plot shows that the temperature at the further end of the thermopile arm changes by 0.6 °C during surface heating, whereas the temperature at the center rises by 6 °C during the same period. The cooling due to the touchdown and the recovery of pad temperature is qualitatively similar to the experimental measurements. A steep rise in temperature results due to sudden application of the heat source. After the initial rise the temperature continues to rise at a very slow rate. The temperature drops after the surface heating is turned off. The rise and drop in temperature are qualitatively similar to the experimental observations and indicate that a finite amount of heat is generated throughout the ultrasonic excitation during bonding. During actual bonding, however, the heat generation is not constant and may not necessarily be confined to surface heating. The

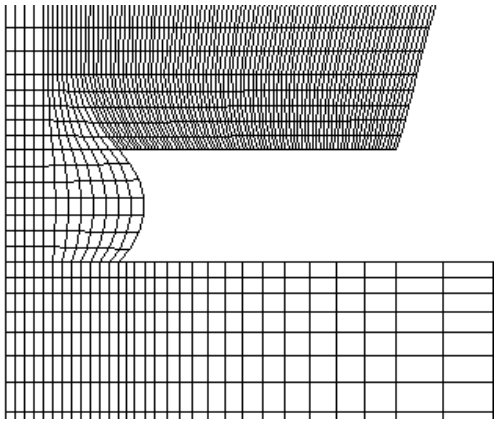

Fig. 7 Mesh near the ball and bond pad interface. Quadrilateral axi-symmetric elements are used for discritizing the domain. The mesh is refined near the ball to capture sharp gradients in temperature.

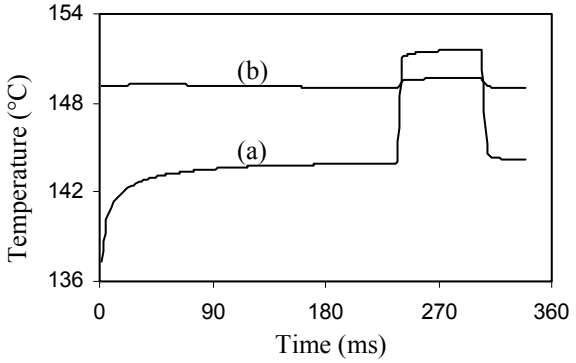

Fig. 8 Temperature at (a) the center of the bond pad and (b) the further end of the thermopile arm.

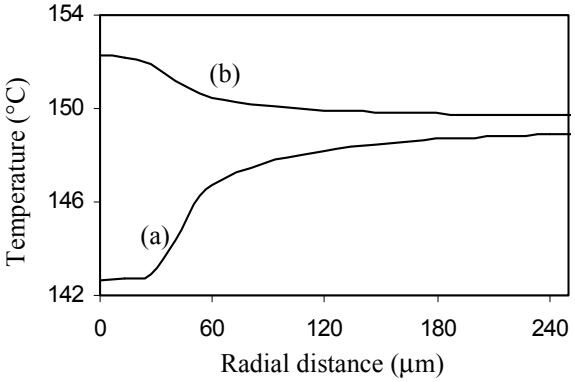

Fig. 9 Temperature at the top surface of chip as a function of the radial distance from the center of the bond pad (a) just before the surface heating is switched on and (b) just before the surface heating is switched off.

contact between the ball and the pad is not uniform and occurs at discrete points where the micro-welds first appear. Also, the total contact area changes due to the deformation of ball and growth of the micro-welds. Once the micro-welds begin to grow and the ball gets pinned, the surface heating probably ceases. A sudden drop in temperature is not observed, which indicates that volumetric heating occurs in the gold ball after the sliding at the bond pad stops. Figure 9 shows the temperature at the top surface of the chip as a function of radial distance at (a) the end of 240 ms (just before the surface heating is switched on), and (b) the end of 305 ms (just before the surface heating is switched off). The temperature at the further end remains close to 150 °C, while the temperature at the center changes depending upon the boundary condition at the bond pad. The temperature is minimum in (a) and maximum in (b) at the center and changes rapidly with the radial distance. The plot shows that the measurements are sensitive to the alignment of the ball on the pad and explains the variability in the measurements due to manual bonding.

Conclusion

A novel thermoelectric device is reported, which can be used to estimate the average temperature at a finite number of points under the bond pad. This can be used along with shear tester results to optimize the bonding force and energy for the wire bonder, based upon the temperature profile during the wire bonding process. A finite element conduction model confirms that a finite amount of heating occurs during the wire bonding process, which stops only after the ultrasonic excitation is switched off.

Disclaimer

Commercial equipment and software referred to in this paper are identified for informational purposes only, and does not imply recommendation of or endorsement by the National Institute of Standards and Technology, nor does it imply that the products so identified are necessarily the best available for the purpose.

Acknowledgement

This work was supported by the NIST Office of Microelectronic Programs.

References

[1] George G. Harman, “Wire Bonding in Microelectronics”, McGraw-Hill Publishers, second edition, Chapter 2, pp. 18-23, 1997.

[2] Michael Mayer, Oliver Paul, Daniel Bolliger, and Henry Baltes, “Integrated Temperature Microsensors for Characterization and Optimization of Thermosonic Ball Bonding Process”, Proceedings of the 1999 Electronic Components and Technology (ECTC), San Diego, California, pp. 463-468, 1999.

[3] Michael Mayer, Oliver Paul, and Henry Baltes, “In-situ Measurements of Stress and Temperature Under Bonding Pads During Wire Bonding Using Integrated Microsensors”, Proceedings of the Second International Conference Microelectronics and Interconnects Technology (EMIT), Bangalore, India, pp. 129-133, 1998.

[4] Adrian Schneuwly, Pierangelo Groning, Louis Schlapbach, and G. Muller, “Bondability Analysis of Bond Pads by Thermoelectric Temperature Measurements”, Journal of Electronic Materials, Vol 27, No. 11. pp. 1254-1261, 1998.

[5] A. Carrass, Victor P. Jaecklin, “Analytical Methods to Characterize the Interconnection Quality of Gold Ball Bonds”, 2nd European Conference of Electronic Packaging Technology (EuPac), Vol 173, pp. 135-139, 1996.

[6] George G. Harman, Kathrine. O. Leedy, “An Experimental Model of the Microelectronic Ultrasonic WireBonding Mechanism”, 10th Annual Proceedings of Reliability Physics, Las Vegas, Nevada, pp. 49-56, 1972.

[7] Martin Von Arx, Oliver Paul, and Henry Baltes, “Test Structures to Measure the Seebeck Coefficient of CMOS IC Polysilicon”, Proceedings of The IEEE International Conference on Microelectronic Test Structures, Vol. 9, March, Trento, pp. 117-122, 1996.

[8] Jurg Schwizer, Michael Mayer, Daniel Bolliger, Oliver Paul, and Henry Baltes, “Thermosonic Ball Bonding: Friction Model Based on Integrated Microsensor Measurements”, IEEE International Electronic Manufacturing Technology Symposium (IEMT), Austin,Texas, October 18-19, pp. 108-114, 1999.